PROCEEDINGS OF SCIENCE

Study of the Photon Strength Function of ^{152}Sm in resonance neutron capture at n_TOF

S. Marrone[1], N. Colonna[*1], M. Krtička[2], U. Abbondanno[3], G. Aerts[4], H. Álvarez-Pol[5], F. Alvarez-Velarde[6], S. Andriamonje[4], J. Andrzejewski[7], P. Assimakopoulos[8], L. Audouin[21], G. Badurek[9], P. Baumann[10], F. Bečvář[2], E. Berthoumieux[4], F. Calviño[13], M. Calviani[26], D. Cano-Ott[6], R. Capote[14,15], C. Carrapico[16], P. Cennini[17], V. Chepel[18], E. Chiaveri[17], G. Cortes[13], A. Couture[20], J. Cox[20], M. Dahlfors[17], S. David[21], I. Dillman[1], C. Domingo-Pardo[11] , W. Dridi[4], I. Duran[5], C. Eleftheriadis[23], M. Embid-Segura[6], L. Ferrant[21], A. Ferrari[17], R. Ferreira-Marques[18], K. Fujii[3], W. Furman[24], I. Goncalves[18], E. Gonzalez-Romero[6], A. Goverdovski[25], F. Gramegna[26], C. Guerrero[6], F. Gunsing[4], B. Haas[27], R. Haight[28], M. Heil[19], A. Herrera-Martinez[17], M. Igashira[29], E. Jericha[9], Y. Kadi[17], F. Käppeler[19], D. Karadimos[8], D. Karamanis[8], M. Kerveno[10], V. Ketlerov[25,17], P. Koehler[30], V. Konovalov[24,17], E. Kossionides[31], C. Lamboudis[8], H. Leeb[9], A. Lindote[18], I. Lopes[18], M. Lozano[15], S. Lukic[10], J. Marganiec[7], C. Massimi[39], P. Mastinu[26], A. Mengoni[14,17], P.M. Milazzo[3], M. Mosconi[19], F. Neves[18], H. Oberhummer[9], S. O'Brien[20], J. Pancin[4], C. Papachristodoulou[8], C. Papadopoulos[33], C. Paradela[5], N. Patronis[8], A. Pavlik[34], P. Pavlopoulos[35], L. Perrot[4], M.T. Pigni[9], R. Plag[19], A. Plompen[36], A. Plukis[4], A. Poch[13], J. Praena[26], C. Pretel[13], J. Quesada[15], T. Rauscher[37], R. Reifarth[28], C. Rubbia[22], G. Rudolf[10], P. Rullhusen[36], J. Salgado[16], C. Santos[16], L. Sarchiapone[17], I. Savvidis[23], C. Stephan[21], G. Tagliente[1], J.L. Tain[11], L. Tassan-Got[21], L. Tavora[16], R. Terlizzi[1], G. Vannini[39], P. Vaz[16], A. Ventura[38], D. Villamarin[6], M. C. Vincente[6], V. Vlachoudis[17], R. Vlastou[33], F. Voss[19], S. Walter[19], H. Wendler[17], M. Wiescher[20], K. Wisshak[19]

The n_TOF Collaboration

[1]Istituto Nazionale di Fisica Nucleare, Bari, Italy; [2]Charles University, Prague, Czech Republic; [3]Istituto Nazionale di Fisica Nucleare, Trieste, Italy; [4]CEA/Saclay - DSM, Gif-sur-Yvette, France; [5]Universidade de Santiago de Compostela, Spain; [6]Centro de Investigaciones Energeticas Medioambientales y Tecnologicas, Madrid, Spain; [7]University of Lodz, Lodz, Poland; [8]University of Ioannina, Greece; [9]Atominstitut der Österreichischen Universitäten, Technische Universität Wien, Austria; [10]Centre National de la Recherche Scientifique/IN2P3 - IReS, Strasbourg, France; [11]Instituto de Física Corpuscular, CSIC-Universidad de Valencia, Spain; [12]Dipartimento di Fisica Generale, Università di Torino, Italy; [13]Universitat Politecnica de Catalunya, Barcelona, Spain; [14]International Atomic Energy Agency, NAPC-Nuclear Data Section, Vienna, Austria; [15]Universidad de Sevilla, Spain; [16]Instituto

[*] Speaker

PoS(PSF07)019

PROCEEDINGS OF SCIENCE

Tecnológico e Nuclear(ITN), Lisbon, Portugal; [17]*CERN, Geneva, Switzerland;* [18]*LIP - Coimbra & Departamento de Fisica da Universidade de Coimbra, Portugal;* [19]*Forschungszentrum Karlsruhe GmbH (FZK), Institut für Kernphysik, Germany;* [20]*University of Notre Dame, Notre Dame, USA;* [21]*Centre National de la Recherche Scientifique/IN2P3 - IPN, Orsay, France;* [22]*Università degli Studi Pavia, Pavia, Italy;* [23]*Aristotle University of Thessaloniki, Greece;* [24]*Joint Institute for Nuclear Research, Frank Laboratory of Neutron Physics, Dubna, Russia;* [25]*Institute of Physics and Power Engineering, Kaluga region, Obninsk, Russia;* [26]*Istituto Nazionale di Fisica Nucleare(INFN), Laboratori Nazionali di Legnaro, Italy;* [27]*Centre National de la Recherche Scientifique/IN2P3 - CENBG, Bordeaux, France;* [28]*Los Alamos National Laboratory, New Mexico, USA;* [29]*Tokyo Institute of Technology, Tokyo, Japan;* [30]*Oak Ridge National Laboratory, Physics Division, Oak Ridge, USA;* [31]*NCSR, Athens, Greece;* [32]*Japan Atomic Energy Research Institute, Tokai-mura, Japan;* [33]*National Technical University of Athens, Greece;* [34]*Institut für Isotopenforschung und Kernphysik, Universität Wien, Austria;* [35]*Pôle Universitaire Léonard de Vinci, Paris La Défense, France;* [36]*CEC-JRC-IRMM, Geel, Belgium;* [37]*Department of Physics and Astronomy – University of Basel, Basel, Switzerland;* [38]*ENEA, Bologna, Italy;* [39]*Dipartimento di Fisica, Università di Bologna, and Sezione INFN di Bologna, Italy.*

E-mail: nicola.colonna@ba.infn.it

The Photon Strength Function of ^{152}Sm has been investigated at n_TOF by studying the γ-ray spectra from resonance neutron capture of ^{151}Sm. The experimental apparatus consisted of two C_6D_6 liquid scintillator detectors. The measured spectra were compared with the predictions of the DICEBOX code, for different assumptions on the Photon Stregth Functions and on the Nuclear Level Density. For a meaningful comparison, the model calculations were filtered through a detailed software replica of the experimental apparatus, performed by means of three different Monte Carlo simulations. Preliminary results indicate that a reasonable reproduction of the experimental γ-ray spectrum is obtained by postulating the presence of a Scissors Resonance. Some hints on the most suitable models, developed in the most recent studies of the Photon Strength Functions and Nuclear Level Density, are also obtained.

Workshop on Photon Strength Functions and Related Topics
Prague, Czech Republic
17-20 June 2007

PoS(PSF07)019

PROCEEDINGS OF SCIENCE

1. Introduction

The study of neutron induced reactions has recently gained a renewed interest in the Nuclear Physics community. Accurate data from neutron studies are needed in Nuclear Astrophysics to improve the knowledge of Stellar Nucleosynthesis of heavy elements in the Universe, which proceeds mainly through neutron capture processes [1]. In addition new concepts in nuclear technology for energy production, radioactive waste transmutation [2] and nuclear medicine applications [3] require accurate new data on neutron cross sections for a variety of isotopes, many of which are radioactive. Neutron studies can also be very useful in fundamental Nuclear Physics studies. Photon Strength Functions (PSF) are among the nuclear properties that can be conveniently investigated in neutron-induced reactions. The advantage in this case consists in the possibility to extend the investigation to energies below the neutron separation energy, as well as to isolate and analyze the spectra from resonances characterized by different quantum numbers, i.e. orbital angular momentum l, spin S, total angular momentum J, and parity. Finally, neutron reactions may allow to investigate nuclei that would be difficult to access with other, more standard methods.

The renewed interest in neutron studies for fundamental and applied Nuclear Physics has recently stimulated the construction of a pulsed white-spectrum spallation neutron source at CERN: n_TOF. The facility, based on the 20 GeV/c proton beam from the Proton Synchrotron (PS), is characterized by a very high instantaneous neutron flux, a high resolution, a low background, and a wide energy range. These features make n_TOF suitable for collecting new and accurate data, in particular on radioactive isotopes. A high performance detectors and a state-of-the-art data acquisition system based on fast Flash ADC have been set-up to match the innovative characteristics of the neutron beam. The n_TOF facility, the experimental apparatus and the DAQ have been described in details in previous publications [4, 5].

The ^{151}Sm(n,γ) reaction was among the first successful measurements performed at n_TOF. This isotope is a β emitter with a relatively short lifetime, $t_{1/2}$=93 yr, so that under stellar conditions a competition exists between neutron capture and β-decay, with the branching ratio depending on the thermodynamic conditions of the stellar site in which the capture process occurs. Its cross-section is therefore important for constraining the temperature during He burning in Asymptotic Giant Branch (AGB) stars. Data on the ^{151}Sm(n,γ) reaction are also important for advanced reactor concepts, where it determines the transmutation rate of this long-lived fission product. Although the sample was highly radioactive (150 GBq), the measurement at n_TOF was characterized by a very large signal-to-background ratio, thanks to the high instantaneous flux of the neutron beam, and the large neutron capture cross-section of ^{151}Sm. The results on the ^{151}Sm(n,γ) cross-sections, and their implications on Nuclear Atrophysics and applications have been reported in Ref. [6, 7].

In consideration of the very high quality data collected at n_TOF, we have recently undertaken a study of the Photon Strength Function for ^{152}Sm. This isotope belongs to a nuclear

PoS(PSF07)019

region where the nuclei undergo a transition from spherical vibrator to axial rotor [8], the deformation of this nucleus being β_2 = 0.243 [9]. Moreover the ^{152}Sm assumes a crucial importance because it is at the critical point of the phase transition. In this particular isotope, the study of low excitation energy levels are able to define the real nature of the transition and to determine the possible presence of some particular symmetries in the Nuclear Structure of those nuclei [10]. The variations of the nuclear properties are expected to influence both the nuclear level density and the Photon Strength Functions. This trend is observed in rare earth nuclei (Nd, Sm, Gd and Dy) for A~150 and is particularly evident in Sm nuclides because of the presence of several stable or long-lived isotopes which span a wide range of atomic masses between 142 and 154. Probably the most important phenomenon from the point of view of decay properties of the deformed nucleus is the so called Scissors Mode. Firstly predicted by Lo Iudice and Palumbo [11] and observed by Bohle et al. [12], the strength of this mode, that significantly influences the decay, is assumed to be proportional to the square of deformation [13]. This dependence comes from Nuclear Resonance Fluoresence (NRF) measurements, but it would be desirable to verify such a dependence in other reactions [14]. The study of ^{152}Sm produced by neutron capture reaction can provide interesting information on the presence of the Scissors Mode, as well as on other features of the PSF at γ-ray energies below the neutron separation energy (B_n=8.258 MeV).

We report here the first attempt to extract information on the Photon Strength Function of ^{152}Sm, by analyzing the γ-ray spectra from resonances in the ^{151}Sm(n,γ) reaction, and comparing them with different model predictions of the radiative decay. The procedure and preliminary results are here described and some conclusions are drawn.

2. Experimental technique

The prompt capture γ-rays were detected with two C_6D_6 liquid scintillation detectors with an active volume of ~1000 cm^3 [15]. The scintillator is contained in a thin-walled carbon fiber cell directly coupled to an EMI 9823 QKA phototube. The detectors are positioned 90 mm upstream of the sample with the front being about 30 mm from the beam axis as shown in the schematic sketch of the setup in Figure 1. The samples were mounted on a remotely controlled carbon fiber sample changer. In this measurement, a 206 mg Sm_2O_3 powder pressed to a solid pellet 10 mm in diameter, sealed inside a canning of natural titanium, was used.

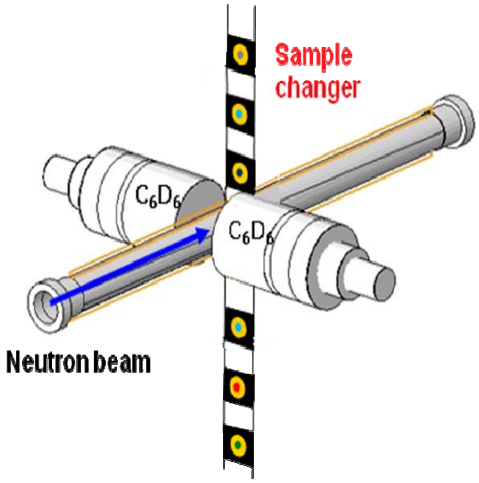

Figure 1: *Sketch of the experimental apparatus used in the measurement.*

PoS(PSF07)019

The sample was chemically purified and prepared at Oak Ridge National Laboratory 2.6 yr prior to the n_TOF measurement. The isotopic composition was determined by mass spectrometry immediately. At the time of the measurement the enrichment of ^{151}Sm was ~88% with respect to the number of samarium and europium atoms while the decay product ^{151}Eu had grown to slightly more than 1.7%. An empty Ti can was used to determine the ambient background. Samples of C, Pb and Au were also measured for determining the various background components and for normalization purposes. More details on the experimental apparatus and data analysis procedure can be found in various publications from the n_TOF Collaboration [16-18].

2.1 Data analysis

The present analysis relies on the accurate determination of the γ-ray spectra for selected neutron capture resonances from the ^{151}Sm(n,γ) reaction. Due to the characteristics of the liquid scintillator, in which the dominant interaction mechanism is Compton scattering, the deposited energy in the detector E_D represents a fraction of the original γ-ray energy $E\gamma$. The resulting spectrum is therefore a convolution of the original γ-ray spectrum with the response of the detector. The poor energy resolution of the C_6D_6 detectors makes it impossible to compare directly the measured spectrum with the prediction of theoretical calculations of the γ-ray cascade. As described later, a different procedure has to be followed, in which the model predictions are filtered through the detector's response before being compared with the experimental results.

Experimental γ-ray spectra have been constructed for selected resonances of the ^{151}Sm(n,γ) reaction. Thanks to the good energy resolution of the n_TOF neutron beam, capture resonances are individually identified, rejecting those related to contaminants in the sample. Figure 2 shows some of the resonances selected in the present analysis. The energy range used in the analysis is between 1 and 400 eV. A further refinement in the analysis consists in the background subtraction. The ambient background and that related to the sample container were measured with an empty Ti-can, and subtracted from the capture events.

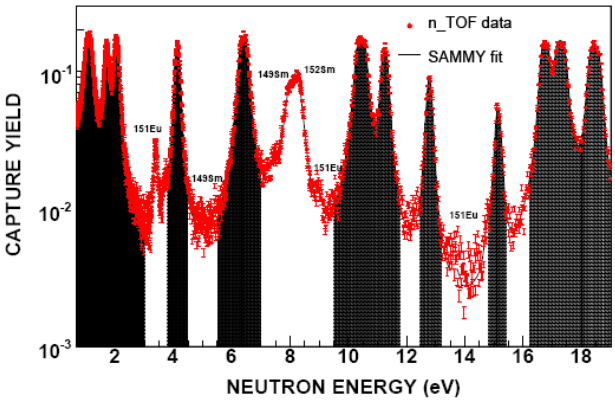

Figure 2: *Capture yield for ^{151}Sm. The filled regions show some selected resonances for the analysis of the ^{152}Sm Photon Strength Functions.*

PoS(PSF07)019

Figure 3 shows the spectra of the energy deposited in the C_6D_6 for the Sm_2O_3 sample and for the Ti-can. As evident in the figure, the background is negligible (two orders of magnitude lower than the capture events) for deposited energies below 5 MeV. At higher energies the signal-to-noise ratio becomes worse, although even at 8 MeV the background is still a factor of two lower than the signal. As mentioned before, the contribution of the sample radioactivity is negligible, thanks to the high instantaneous neutron flux of n_TOF. The residual contribution, dominated by low energy γ-rays ($E_\gamma < 50$ keV), is suppressed by the applied threshold. The background from neutrons scattered by the sample and captured in or near the detectors was estimated by means of the carbon sample, and was found to be negligible, as expected from the low neutron sensitivity of the experimental set-up (see Ref. [7] for more details). Another background component, associated to in-beam γ-rays scattered by the sample, was investigated by means of a ^{nat}Pb sample. In this case, a sizable background is observed only for neutron energies above 1 keV, while in the energy region here considered this component is negligible.

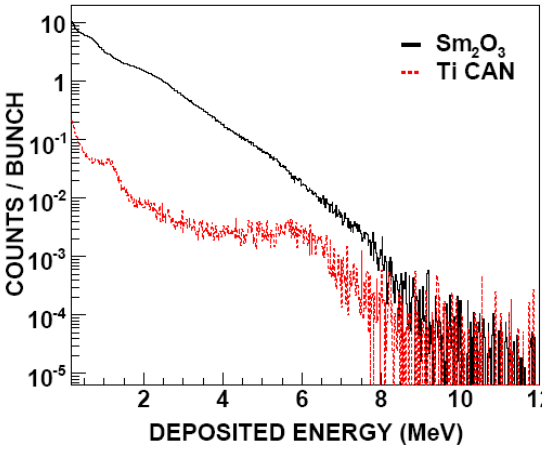

Figure 3: *Measured γ-ray spectrum in the C_6D_6 detectors, corresponding to the ^{151}Sm(n,γ) resonances between 1 and 400 eV. The red histogram represents the background estimated with an empty Ti can, similar to the one enclosing the sample.*

In order to compare the experimental results with the model prediction, the measured γ-ray spectra were normalized to the total number of capture events selected in the analysis. To this end, we have used the official n_TOF neutron flux, measured with different systems to an accuracy of 3 % [5]. Since the sample was smaller than the beam profile, only a fraction of neutron beam concurs to the capture reactions. This fraction was estimated from a sample of Au of the same dimensions, by analyzing the standard 4.9 eV resonance in the Au(n,γ) reaction. The SiMon detector [19] was used for relative normalization of the neutron fluence between different samples. A correction was also applied to account for the dead-time of the detector, which amounts to ~1 % only for the strongest resonances.

The calibration of the deposited energy was performed with three γ-ray sources: ^{60}Co, ^{137}Cs and Pu/C, and periodically checked during the measurement with the same sources.

3. Model predictions

Despite the fact that the measured γ-ray spectrum from C_6D_6 detectors is heavily affected by the poor resolution of the detector, it may still carry valuable information about the decay

PoS(PSF07)019

properties of this nucleus. To this end, we have performed a comparison of the measured spectrum with the results of theoretical models using different assumptions on the Photon Strength Functions (PSF) and the Nuclear Level Density (NLD). The model calculations are subsequently filtered through the response of the detection apparatus, to account for the efficiency and experimental resolution. Finally, the filtered model predictions are compared with the measured γ-ray spectrum to obtain information on the most appropriate PSD and NLD models for the nucleus under investigation.

Artificial decay spectra of ^{152}Sm were simulated using the DICEBOX algorithm [20]. This algorithm simulates decay within the extreme statistical model, embodying Bohr's idea of a compound nucleus [21], the paradigm of fragmentation of photon strength [22] and validity of the Brink hypothesis [23, 24]. The decay of highly excited nuclear states can be described in terms of two entities: (i) a set of PSFs for various types of multipolarities of the emitted radiation, and (ii) the NLD as a function of excitation energy and spin. A detailed description of the PSF and NLD models used in the DICEBOX simulations can be found elsewhere [25]. In brief, several combinations of different models for the PSF and for the NLD were tested, with different assumptions on some of the parameters.

Three contributions were considered for the Photon Strength Function, related to the dipole (E1) and quadrupole (E2) electric transition and to the dipole magnetic momentum (M1). The E1 transition, which dominates the PSF, is closely linked to the Giant Dipole Electric Resonances (GDERs), built in accordance with the Brink hypothesis on the ground state, as well as on each excited nuclear level. From rich photonuclear data it is known that the ground-state GDERs of the vast majority of the medium-weight and heavy nuclei at γ-ray energies above the neutron binding energy are described by a Lorentzian above neutron separation energy [26]. In transitional and deformed nuclei the Lorentzian splits into two components. In this formalism, the E1 PSF is written in terms of the energy E_G, damping width Γ_G and maximum of the photonuclear cross-sections σ_G of the two individual components of the GDER. In the present work, the following values were adopted for ^{152}Sm [26]: $E_G = 12.38$ MeV, $\Gamma_G = 2.97$ MeV, and $\sigma_G = 176$ mb for the lower component, and $E_G = 15.74$ MeV, $\Gamma_G = 5.22$ MeV, and $\sigma_G = 234$ mb for the higher component of the GDER. A natural question arises in the present analysis, whether the Lorentzian shape remains a reasonable approximation also below the neutron separation energy of ^{152}Sm at $B_n = 8.258$ MeV. Due to experimental limitations, the shape of the GDERs at energies $E_\gamma < B_n$, cannot be easily determined in a straightforward way from the photoabsorption experiments, let alone the case of the GDERs built on excited levels, where these limitations are in principle insurmountable. Some data on the intensity of primary transitions from (n,γ) reactions with slow neutrons, collected for ^{148}Sm and ^{150}Sm [27, 28], indicated that the Brink-Axel model is probably not completely valid at energies below the neutron separation energy in spherical and transitional nuclei. These data spoke rather in favor of a model proposed by Kadmenskij, Markushev and Furman (KMF) [29] who worked it out using microscopic calculations within the frame of the semi-microscopic shell model approach,

PoS(PSF07)019

based on the results of the theory of Fermi liquids. Their expression depends on the excitation energy of a final level, the pairing energy and the shell-model Liquid Drop parameter. This model was derived for spherical nuclei and it can be taken only as a low-energy approximation of the E1 PSF as it diverges for $E_\gamma = E_G$. It is not clear how this model would perform when applied to transitional and deformed nuclei. In order to describe spherical and deformed nuclei within one model and to remove at the same time the divergence in the KMF model, Kopecky and collaborators suggested the phenomenological Enhanced Generalized Lorentzian (EGLO) model [30]. In this work, the same values for the parameters E_G, Γ_G and σ_G were used in the KMF and EGLO models, as in the BA model. Another model that connects the low-energy behavior given by the KMF model with the BA model at higher energies was suggested in Ref. [31]. This model (referred here as the BA+KMF models) employs the KMF model for γ-ray energies below a chosen value E_L and the BA model above an energy E_H. In between these energies the PSF is expressed as a linear combination of the BA and KMF strength functions. An analysis of several deformed nuclei in [31] led to the conclusion that reasonable values for E_L and E_H are 4.0 MeV and 8.0 MeV, respectively. Figure 4 shows the E1 Photon Strength Functions calculated with the different models.

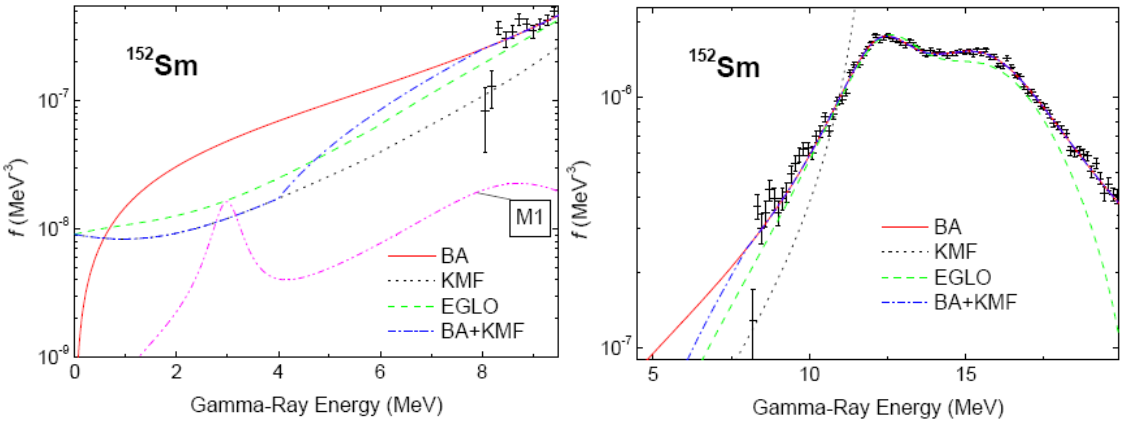

Figure 4: *Photon Strength Functions calculated with different models. The symbols refer to photonuclear experimental data.*

For the M1 photon strength functions, we have used two widely employed models: the Single Particle (SP) and Spin-Flip (SF) model. According to the SP model the M1 PSF is energy independent, while in the SF model the strength functions is assumed to be described by a resonance structure, with Lorentzian shape, with parameters E_{SF} = 8.95 MeV and Γ_{SF} = 4 MeV. The last parameter σ_{SF} is determined considering data for neighboring nuclei or from the ratio of the E1 and M1 strength functions. Both these approaches can be applied also for determining the constant value of the M1 PSF in the case of the SP model. The SF model predicts very small M1 strength for Eγ < 5 MeV. Analysis of several nuclei with 95 < A < 170 using the method of Two-Step Cascades showed that this is probably not fully correct and that the M1 strength plays

PoS(PSF07)019

a non-negligible role at lower γ-ray energies [31, 32]. There are some indications that a "composite" model, in which a SF resonance term is combined with a SP "background", might be a good description for spherical nuclei. In transitional and deformed nuclei an additional resonance term, known as the Scissors Resonance (SR) should occur near 3 MeV. The strength of this mode is believed to be scaled with the square of the deformation of the nucleus. As ^{152}Sm is almost well deformed this mode should play an important role in the decay of this nucleus. According to the phenomenological sum-energy rule [33] the total strength of this mode built on the ground state in well-deformed even-even nuclei is about $3\mu^2_N$. This strength was observed also in many NRF experiments [34] - for ^{152}Sm it was $2.26(9)\mu^2_N$ between 2.7 and 3.7 MeV [34, 35] - although this value is in disagreement with that derived from the analysis of Two-Step Cascades spectra in odd ^{163}Dy [36] where it was about $6\mu^2_N$. The shape of the SR is again often described as a Lorentzian, with a set of parameters E_{SR} (~ 3 MeV) $\Gamma_{SR} = 0.6$ MeV [36] and σ_{SR} ~ 0.5 mb which yield a total strength of $3\mu^2_N$.

For the E2 photon strength function, the single particle model was used in the calculations with the value of 10^{-10} MeV^{-5} (see Ref. [28]). Finally, for the Nuclear Level Densities, we have used two common, parity-independent expressions: the Constant Temperature Formula (CTF), and the back-shifted Fermi Gas (BSFG) model [37]. For ^{152}Sm, the values of the parameters entering in the nuclear density expressions were determined from systematics [38]. The following parameters were adopted in the CTF model for the level density parameter *a*, temperature *T* and E_0: a = 18.57 MeV^{-1}, T = 0.559 MeV, E_0 = -0.37 MeV. For the BSFG, E_1 was set to 0.37 MeV, while the prescription of Ref. [39] was used for the spin cut-off factor.

4. Discussion and results

The γ-ray cascade for ^{152}Sm, following neutron capture on ^{151}Sm, were generated with the DICEBOX code for different combinations of the E1, E2 and M1 photon strength function, as well as for the two choices of the Nuclear Level Density. For each set of PSFs and NLD, 10^6 capture cascades in ten different nuclear realizations were generated [20]. The cascades were then filtered through the experimental setup by means of Monte Carlo simulations. Three different Monte Carlo tools were used for this purpose, namely GEANT-3.21 [40], GEANT-4 [41] and MCNP [42]. For each of them, a detailed software replica of the experimental apparatus was implemented, carefully reproducing the experimental geometry and the various material. The γ-ray cascade was generated uniformly inside the sample and according to the beam profile. The purpose of using three different Monte Carlo simulations was to gain a high degree of confidence on the reliability of the results. In fact, as a first step of the analysis, it was checked that simulations performed with the three different codes for the same nuclear cascade gave very similar results. This was found to be the case in the whole energy range, except for a small difference around 500 keV, most probably due to minor differences in the implementation

PoS(PSF07)019

of the beam line around the sample, which enhanced in some case the interaction of emitted γ-rays by pair production. The observed differences are however small and do not affect the conclusions of the present work. The generally good agreement between the three Monte Carlo codes therefore provided confidence on the reliability of the simulations. A check was also performed to ensure that the results did not depend on the nuclear realization. Finally, we have investigated the effect of the choice of the resonance spin *J*. Experimental information about spins of individual resonances is not available in this measurement. However, the statistical analysis, reported in the Ref.[7], evidenced that all resonances detected up to 400 eV neutron energy have likely orbital angular momentum $l = 0$. Capture of s-wave neutrons on the $J^{\pi} = 5/2^{+}$ ground state of ^{151}Sm can form $J^{\pi} = 2^{+}$ or 3^{+} resonances in the compound nucleus ^{152}Sm. The statistics is too low to observe any significant difference among spectra from individual resonances. Nevertheless, the effect of the total spin on the γ-ray spectrum was studied by means of simulations, by comparing the theoretical γ-ray spectra for two different assumptions on the resonance spin *J*. The model predictions, filtered through the experimental set-up with GEANT-3.21, did not show appreciable differences in the final spectra. In any case, for the comparison with experimental spectra, both capturing states were produced in the model calculations, and mixed together with weights given by the statistical spin probability distribution function (spin cut-off σ_C=0.98A$^{0.29}$). As the influence of the resonance spin on the γ-ray spectra is negligible, a more realistic spin distribution is not necessary in this work.

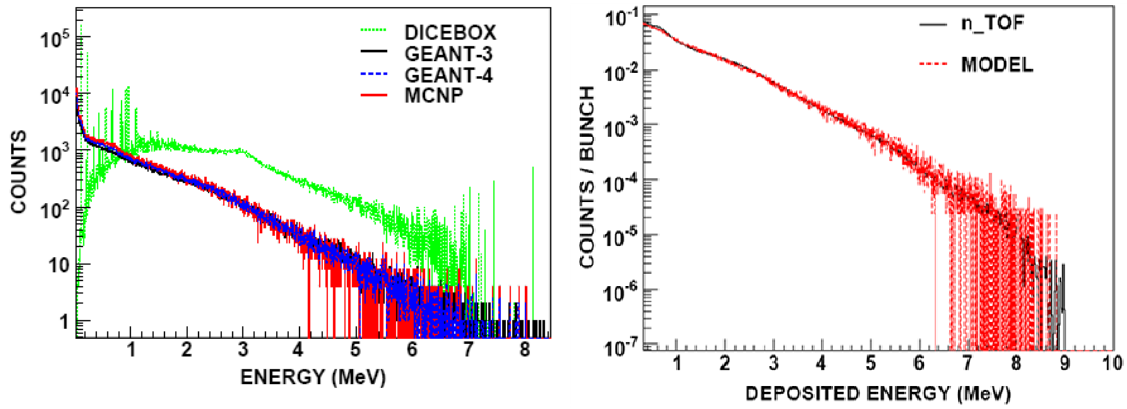

Figure 5: *Left panel: calculated γ-ray spectrum from the decay of ^{152}Sm formed in the ^{151}Sm(n,γ) reaction (green histogram). The spectra obtained after filtering through the response of the experimental apparatus with three different Monte Carlo codes are also shown in the figure (black, blue and red histogram). Right panel: a comparison between the experimental data (black histogram) and model calculations (in red). A small bump is observed between 2 and 3 MeV, probably related to the presence of the scissors mode in the PSF for this nucleus.*

The γ-ray spectra obtained from the simulations were finally compared with the measured spectra in the ^{151}Sm(n,γ) reaction, obtained from the sum of the γ-ray spectra for all resonances

PoS(PSF07)019

below 400 eV. The experimental and the simulated data are normalized to the same number of captured neutrons. Some combinations of the different PSF models could be immediately discarded by the visual comparison between predicted and measured spectra. The left panel of Figure 5 shows the original γ-ray spectrum generated with DICEBOX, for a reasonable choice of the PSF and NLD models, and the one obtained after filtering the model predictions through the experimental apparatus, with the three Monte Carlo codes used in the present analysis. In the right panel, the filtered predictions are compared with the measured γ-ray spectrum. Good agreement is generally observed at higher energy for most of the models. The study of all possible combinations has led us to conclude that the most sensitive region for comparison, in the present analysis, is below 4 MeV. A feature that can be observed in the experimental spectrum is a small bump at around 2.5 MeV. This evidence speaks in favor of the presence of the Scissors Resonance, since the bump is reproduced by the model calculations only when the SR is included in the model calculations.

In Figure 6 two cases are shown in which different model predictions are compared with the experimental data: in the left panel, the KMF model was used for E1, the SF for M1, to which a Scissors Resonance was added, and the BSFG model for the nuclear level density. As evident, the agreement is quite poor up to 2 MeV (although it improves at higher energy).

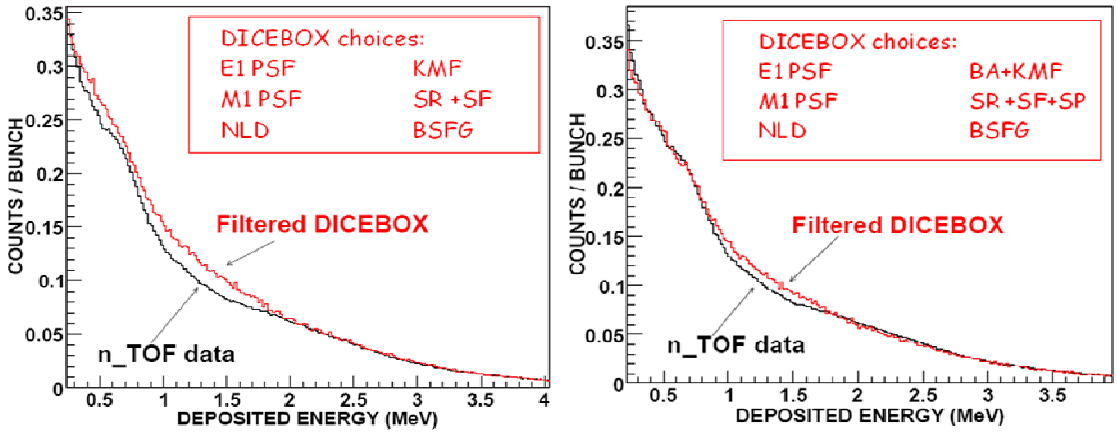

Figure 6: *The experimental spectrum (black histogram) is compared with two different model calculations (red histograms). An improved agreement with the measured spectra is obtained by using the BA+KMF model for the E1 PSF and adding a constant term in M1. The presence of the Scissors Resonance is necessary in both cases to reproduce the behavior of the measured spectrum around 2.5 MeV.*

We have observed that in this case, the use of the BA, the KMF or EGLO models for E1, lead to predicted spectra that do not agree well with the measured ones. We have also observed that the agreement with the experiment is generally better when using the BSFG model for the NLD, rather than the CTF one. However, this cannot be taken as evidence that BSFG model is

PoS(PSF07)019

more reliable, since the shape of the γ-ray spectrum is a rather complicated interplay between the NLD and PSFs.

In the right panel, the theoretical cascades were generated with other sets of PSF and NLD models: for the E1 PSF the BA+KMF model was used; for M1 the SF model was combined with a constant SP background, and with a SR of total strength $3\mu^2_N$, while the BSFG model was used for calculating the nuclear level density. In this case, the agreement is much better. The presence of the Scissors Resonance with strength 3 to $6\mu^2_N$ leads in general to an improved reproduction of the experimental result, thus providing a hint of the importance of the Scissors mode in this deformed nucleus. We have also observed that the introduction of a constant background in M1 helps in obtaining better agreement between the model predictions and the measured spectra.

While some preliminary conclusions can already be drawn on the PSF and, in particular, on the presence of the Scissors Resonance, a more refined analysis is currently in progress, in which a quantitative comparison is performed by calculating the reduced χ^2 between the filtered model predictions and the experimental γ-ray spectra. Furthermore, a comparison is also performed for the average radiation width of the capture resonances Γ_γ, which for ^{152}Sm was experimentally found to be 95(4) meV.

5. Conclusions

This paper reports on a first attempt to investigate the Photon Strength Function of ^{152}Sm, by studying the γ–ray spectrum measured in neutron capture on ^{151}Sm. The measurement was performed at the innovative neutron time-of-flight facility at CERN, with C_6D_6 liquid scintillator detectors. The aim of the present work was to gain information on the Photon Strength Functions and the Nuclear Level Densities of deformed nuclei in the transitional region. Model calculations performed with DICEBOX, and filtered through the response of the experimental set-up by means of Monte Carlo simulations have been compared with the experimental spectra of selected resonances in the capture yield of ^{151}Sm. Thanks to the excellent features of the n_TOF facility, it has been possible to obtain experimental spectra with very low-background. The results, though preliminary, indicate the presence of a Scissors Resonance in M1. A combination of models for the E1 Photon Strength Functions is also found to be more appropriate to reproduce the data. A further analysis, based on a more quantitative comparison of the model predictions and experimental results, currently in progress, may be useful to put some constraints on the model parameters.

This work is the first of a series of studies that can be performed on other isotopes measured at n_TOF. The high instantaneous neutron flux of the neutron beam and the excellent background conditions are of great advantage for studies of the Photon Strength Function below the neutron separation energy, in particular for nuclei that would be difficult to investigate with

PoS(PSF07)019

other methods. A disadvantage of the method presented here is related to the characteristics of the experimental set-up. In fact the low efficiency and the poor energy resolution of the liquid organic scintillator, used in some neutron capture measurements, are strongly limiting the quality and the predictive power of the measured γ-ray spectra. This problem is to a large extent overcome with the use of the BaF_2 total absorption calorimeter (TAC) [43, 44], which was set in operation in the last part of the measurement campaign at CERN, and that will allow more dedicated studies of the PSF in the future.

References

[1] F. Kaeppeler, Prog. Nucl. Part. Phys. **43**, 419 (1999).

[2] C. Rubbia et al., CERN/AT/95-53 (1995).

[3] E. Bisceglie et al., Phys. Med. Biol. **45**, 49 (2000).

[4] n TOF Collaboration, Status Report, CERN-INTC-2001-021 (2001).

[5] n TOF Collaboration, Performance Report, CERN-INTC-O-011 (2003).

[6] U. Abbondanno et al., Phys. Rev. Lett. **93**, 161103 (2001).

[7] S. Marrone et al., Phys. Rev. **C73**, 034604 (2006).

[8] R. F. Casten and N. V. Zam_r, Phys. Rev. Lett. **87**, 052503 (2001).

[9] P. Moller et al., At. Data and Nucl. Data Tables **59**, 185 (1995).

[10] R. F. Casten, Nature Physics **2**, 811 (2006).

[11] N. LoIudice and F. Palumbo, Phys. Rev. Lett. **41**, 1532 (1978)

[12] D. Bohle et al., Phys. Lett. B **137**, 27 (1984).

[13] N. Pietralla, Phys. Rev. **C58**, 184 (1998).

[14] J. Zawischa, Journ. Phys. G **24**, 683 (1998).

[15] R. Plag et al., Nucl. Instr. Methods A **496**, 425 (2003).

[16] U. Abbondanno et al., Nucl. Instr. Methods A **521**, 454 (2004)

[17] G. Aerts et al., Phys. Rev. **C73**, 054610 (2005).

[18] C. Domingo-Pardo et al., Phys. Rev. **C74**, 025807 (2006) and reference therein.

[19] S. Marrone et al., Nucl. Instr. Methods A **517**, 389 (2004).

[20] F. Bečvar, Nucl. Instr. Methods A **417**, 434 (1998).

[21] N. Bohr, Nature **137**, 344 (1936).

PoS(PSF07)019

[22] G. A. Bartholomew, Ann. Rev. of Nucl. Sci. **11**, 259, (1961).

[23] D. M. Brink, Ph.D. Thesis, Oxford University, 1955.

[24] P. Axel, Phys. Rev. **126**, 671 (1962).

[25] S. Marrone et al., in preparation

[26] S. S. Dietrich and B. L. Berman, At. Data and Nucl. Data Tables **38**, 199 (1988).

[27] F. Bečvar et al., Yad. Fiz. **46**, 3 (1987).

[28] Reference Input Parameter Library for theoretical calculations of nuclear reactions, see http://www - nds.iaea.org/ripl/

[29] S. G. Kadmenskij, V. P. Markushev and V. I. Furman, Sov. J. Nucl. Phys. **37**, 165 (1983).

[30] J. Kopecky, M. Uhl, and R.E. Chrien, Phys. Rev. **C47**, 312 (1993)

[31] M. Krtička, Ph.D. thesis, Charles University in Prague (2002)

[32] L. Zanini et al., Phys. Rev. **C68**, 014320 (2003)

[33] N. LoIudice, A. Richter, Phys. Lett. B **304**, 193 (1993)

[34] U. Kneissl, H.H. Pitz, A. Zilges, Prog. Part. Nucl. Phys. **37**, 349 (1996)

[35] W. Ziegler et al., Phys. Rev. Lett. **65**, 2515 (1990); Nucl. Phys. **A564**, 366 (1993)

[36] M. Krtička et al., Phys. Rev. Lett. **92**, 172501 (2004)

[37] T. D. Newton, Can. J. Phys. **34**, 804 (1956).

[38] T. von Egidy, H. H. Schmidt and A. N. Behkami, Nucl. Phys. **A481**, 189 (1988).

[39] A. Gilbert and A. G. W. Cameron, Can. J. Nucl. Phys. **43**, 1446 (1965).

[40] GEANT, Detector Description and Simulation Tool, CERN Program Library W5013 (1994).

[41] S. Agostinelli et al., Nucl. Instr. Methods A **506**, 250 (2003).

[42] J. F. Briesmeister editor, LA-13709-M (2000).

[43] M. Heil et al., Nucl. Instr. Methods A **459**, 229 (2001)

[44] D. Cano-Ott et al., AIP Conference Proceedings **769**, 1442 (2004)

PoS(PSF07)019

